

PCCP

Accepted Manuscript



This is an *Accepted Manuscript*, which has been through the Royal Society of Chemistry peer review process and has been accepted for publication.

Accepted Manuscripts are published online shortly after acceptance, before technical editing, formatting and proof reading. Using this free service, authors can make their results available to the community, in citable form, before we publish the edited article. We will replace this *Accepted Manuscript* with the edited and formatted *Advance Article* as soon as it is available.

You can find more information about *Accepted Manuscripts* in the [Information for Authors](#).

Please note that technical editing may introduce minor changes to the text and/or graphics, which may alter content. The journal's standard [Terms & Conditions](#) and the [Ethical guidelines](#) still apply. In no event shall the Royal Society of Chemistry be held responsible for any errors or omissions in this *Accepted Manuscript* or any consequences arising from the use of any information it contains.

1 **Voltammetric study of the boric acid-salicylaldehyde-H-acid ternary system and its application**
2 **to the voltammetric determination of boron[†]**

3

4 Mari Kajiwara,^a Yoshio N. Ito,^a Yoshinobu Miyazaki,^b Takao Fujimori,^c Kô Takehara^a and Kazuhisa
5 Yoshimura^{a*}

6

7

8

9

10

11

12

13

14

15

16

17

18 ^a Department of Chemistry, Faculty of Sciences, Kyushu University, Hakozaki, Fukuoka 812-8581,
19 Japan. E-mail: kazz@chem.kyushu-univ.jp

20 ^b Department of Chemistry, Fukuoka University of Education, Akamabunkyo-machi,
21 Munakata, Fukuoka 811-4192, Japan

22 ^c Department of Chemical Science and Engineering, National Institute of Technology, Miyakonojo
23 College, Yoshio-cho, Miyakonojo, Miyazaki 885-8567, Japan

24

25 [†] Electronic supplementary information (ESI) available. See DOI:

26

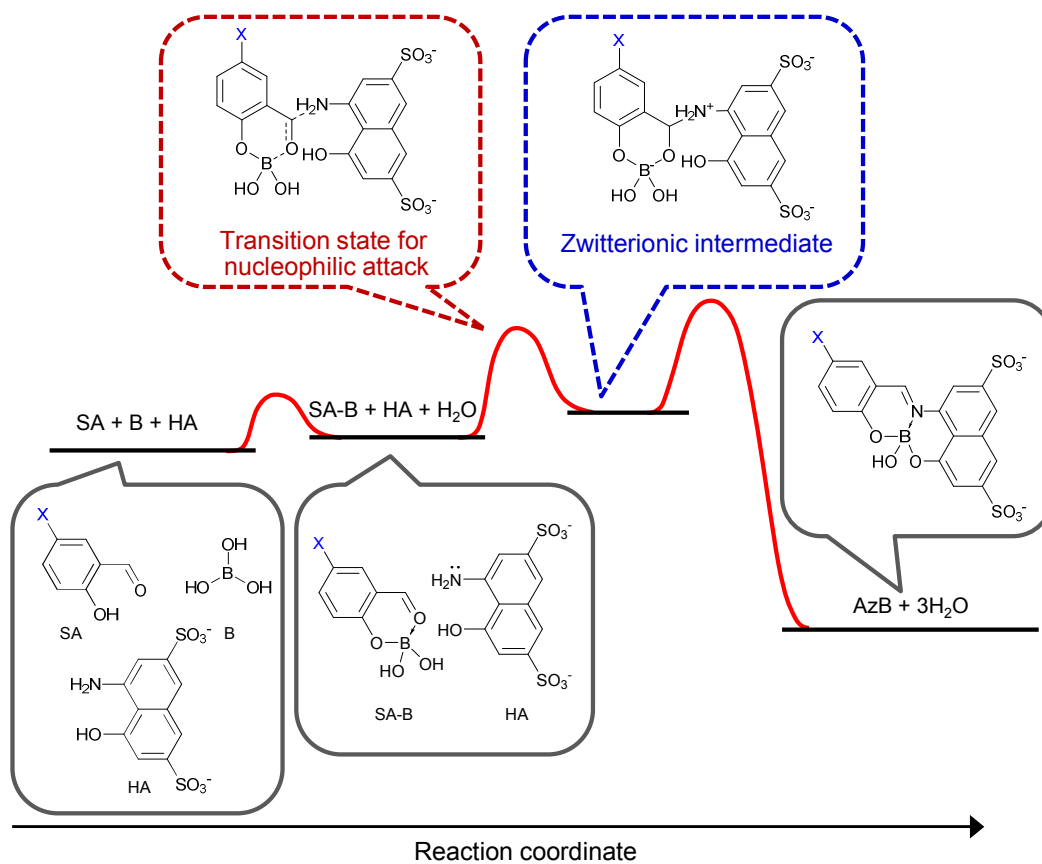
27

28 **Tables of contents entry**

29

30 We fully elucidated the three-component reaction kinetics and thermodynamics of a boric acid

31 complex with H-acid and salicylaldehydes by voltammetry and NMR spectroscopy.



32

33 Abstract

34 The ternary system of boric acid, salicylaldehyde (SA) and H-acid (HA) was voltammetrically
35 studied from kinetic and equilibrium points of view. The effect of the SA substituents was also
36 studied by using two analogs, 5-fluorosalicylaldehyde (F-SA) and 5-methylsalicylaldehyde
37 (Me-SA). The three cathodic peaks of Azomethine H (AzH), Azomethine H-boric acid complex
38 (AzB), and free SA were observed in the solution containing boric acid, SA and HA. The peak
39 potentials of AzH and SA were shifted negative with the increasing pH, while that of AzB was
40 pH-independent. This difference indicates that a proton participates in the charge-transfer steps of
41 the AzH and SA reductions, but not in that of the AzB reduction. The formation constants for the
42 AzB complexation were similar among all the examined analogs. In the kinetic study, the reaction
43 rate was higher in an acidic condition for the AzH formation, whereas in a neutral condition for the
44 AzB formation. The rate constants for the AzB complexes were in the order of F-SA > SA \approx Me-SA,
45 indicating that the fluoro group accelerates the F-AzB complexation. The AzB complexation
46 mechanism is considered to consist of more than three steps; *i.e.*, the pre-equilibrium of the
47 salicylaldehyde-boric acid complex (SA-B) formation, the nucleophilic attack of HA on SA-B, and
48 remaining some steps to form AzB. Based on these results, the voltammetric determination method
49 of boron using F-SA was optimized, which allowed the boron concentration to be determined only
50 within 5 min with a 0.03 mg B dm⁻³ detection limit.

51

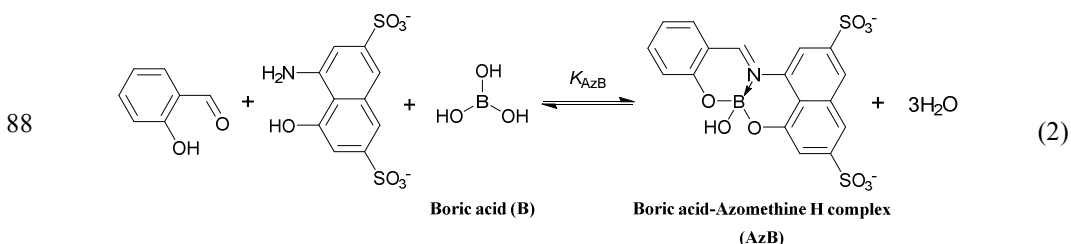
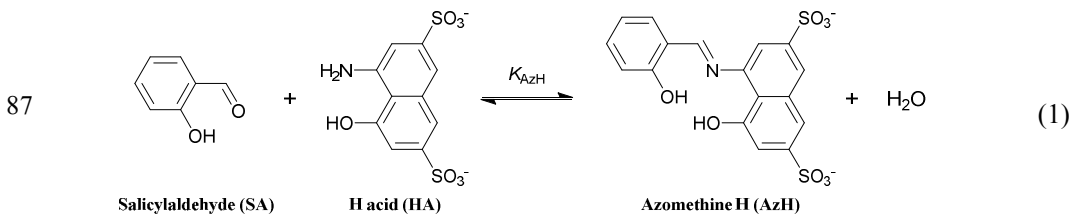
52 Introduction

53 Boron mainly exists as boric acid or the borate anion. Boric acid acts as a Lewis acid to produce the
54 borate anion, accepting the electron pair of a hydroxide ion [1]. It is well-known that boron produces
55 chelate complexes by interactions between the borate and polyol compounds [2-6]. The
56 complexation reaction of borate with polyol is characterized by the dehydration condensation
57 reaction between the alcoholic hydroxyl groups of polyol and the hydroxyl groups of borate to give

58 mono and bischelate complexes. In the case of the acidic polyol, boric acid accepts an electron pair
59 through the nucleophilic attack of the dissociated ligand, followed by a condensation reaction to
60 form the 1:1 monochelate complex. The monochelate complex then reacts with the ligand through
61 the condensation reaction to give the 1:2 bischelate complex [7-9]. For the development of
62 adsorbents selective to boron and analytical methods of boron, reactions between the borate and
63 various polyol compounds have been studied [10-16].

64 On the other hand, in the field of boron analysis, the boron concentration in water is
65 determined by various methods as reviewed by Sah and Brown [17] and by Yoshimura *et al.* [18].
66 Among them, a significant number of spectrophotometric studies have focused on the development
67 of methods which enable one to determine the concentration of boric acid in an aqueous solution
68 under moderate conditions. The Azomethine H method, proposed by Capelle in 1964 [19], has been
69 employed for the boron analyses of natural and waste waters, soils and plants [20-22]. Azomethine
70 H (AzH, 8-hydroxy-1-(salicylideneamino)-3,6-naphthalenedisulfonic acid) is a Schiff base of
71 salicylaldehyde (SA) and H-acid (HA, 1-amino-8-naphthol-3,6-disulfonic acid), and its solution
72 exhibits an absorption maximum at 412 nm in the presence of boric acid. Different from polyols
73 and acidic polyols, the interaction between boric acid and AzH has not been well understood,
74 although a number of studies have been performed for the optimization of conditions for boron
75 determination using AzH as a coloring agent. It has been pointed out in some papers that AzH
76 reacts with boric acid to form chelate complexes in solution, and then the complexes exhibit an
77 absorption maximum in the visible region. Some possible complexes were a 1:1 monochelate
78 complex of trigonal boric acid, a 1:1 bischelate complex with tetrahedral boron, a 1:1 monochelate
79 complex with tetrahedral boron, and its corresponding 1:2 complex [23]. On the contrary, Harp had
80 suggested that the absorption maximum is due only to the AzH species [24]. Direct evidence
81 regarding the coloring processes and the structure of the borate complex has not been provided
82 until our ^{11}B NMR study [23]; ^{11}B NMR spectroscopy provided direct evidence that boric acid

83 reacts with AzH to form a 1:1 bischelate complex (AzB) with a new peak due to the chelate
 84 complex containing tetrahedral boron. It has been quantitatively confirmed that the reaction
 85 includes two chemical equilibria; one is related to the ligand formation and the other to the complex
 86 formation, as shown by the following equations.



89 The formation constant for the ligand is low, whereas that for the complex is relatively high. AzH
 90 is hydrolyzed in an aqueous solution due to its low stability, and the ligand formation is responsible
 91 for the nature of its complexation with boric acid.

92 The electrochemical determination is an easy and simple method, however, it cannot be
 93 applied to the direct determination of boron because boron usually exists as an electrochemically
 94 inactive form in solutions. Alternatively, the complexation of boric acid with an electroactive ligand
 95 can be applied to the electrochemical determination of inert boric acid by voltammetry through the
 96 change in the redox potentials of the ligand by complexation with boric acid [25]. We recently
 97 reported the voltammetric determination of boron using the boric acid-AzH system [26]. The
 98 cathodic peak of the SA, dissociated from the AzH reagent, affects the peak current of the target
 99 complex in the voltammograms, and therefore, the concentration of SA was carefully chosen as low
 100 as possible unless it affects the formation of AzB; *i.e.*, the complexation degree could be kept
 101 constant if the product of the concentrations of SA and HA was maintained constant, and the free

102 SA concentration was reduced by increasing the electrochemically inactive HA concentration. The
103 unique dissociation-formation characteristics of AzH should provide a novel approach to design a
104 voltammetric method optimized for the determination of boric acid using AzH.

105 Elucidation of the complexation mechanism is important to improve the condition for
106 boron determination using AzH by not only voltammetry, but also by spectrophotometry. The AzB
107 complexation between AzH and boric acid is not very fast for practical use. One of the purposes of
108 this study was to clarify the boric acid-SA-HA system from kinetic and equilibrium points of view
109 by combination of the voltammetric and ^{11}B NMR studies. We also clarified the effect of the
110 substituent groups of salicylaldehyde on the AzB complexation using 5-fluorosalicylaldehyde
111 (F-SA) and 5-methylsalicylaldehyde (Me-SA) instead of SA. Based on the determined properties,
112 the voltammetric determination of boron using the boric acid-SA-HA system could be done within
113 5 min.

114

115 **Experimental**

116 **Chemicals**

117 All chemicals, except for boric acid, F-SA, Me-SA, and HA, were of analytical reagent
118 grade and used without further purification. Deionized water prepared by a Milli-Q system
119 (Millipore, USA) was used throughout the study. A boric acid solution was prepared by diluting the
120 $1000 \text{ mg B dm}^{-3}$ boron standard solution (Wako, Japan). A 0.05 mol dm^{-3} aldehyde solution was
121 prepared by dissolving SA (Wako, Japan), F-SA (purity > 98.0%, Tokyo Chemical Industry, Japan)
122 or Me-SA (purity > 98.0%, Tokyo Chemical Industry, Japan) in ethanol. The HA
123 (8-amino-1-naphthol-3,6-disulfonic acid) was a reagent grade monosodium salt (Wako, Japan) and
124 was used without further purification. The purity of HA was determined by acid-base titration of
125 the amino group of HA to be $87.8 \pm 1.6 \%$ ($n = 4$). The rest is reported to be mainly water. The pH
126 of the solution was adjusted using acetate (pH 4 – 6), phosphate (pH 6 – 8), and carbonate (pH 9)

127 buffer reagents. An excess of sodium hydroxide (Wako, Japan) was added to the buffer solution in
128 order to neutralize HA. Sodium chloride (Wako, Japan) was added to adjust the ionic strength at 0.5
129 mol dm⁻³.

130

131 **Determination of acid dissociation constants of salicylaldehyde derivatives and HA**

132 The acid dissociation constants were calculated according to the absorption spectra of the 3.7
133 × 10⁻⁴ mol dm⁻³ respective aldehyde derivative solutions measured at pH 1.76 – 8.99 and of 3.5 ×
134 10⁻⁴ mol dm⁻³ HA solutions at pH 0.49 – 8.62. A U-3500s spectrophotometer (Hitachi, Tokyo) was
135 used for the measurements. All the solutions were prepared under a nitrogen gas for avoiding the
136 oxidation of reagents by oxygen. The ionic strength of the solutions was adjusted to 0.5 mol dm⁻³
137 using NaCl. The pH measurements were done using a Horiba pH meter, F-22 (Kyoto, Japan) with
138 a glass electrode. The dissociation constants of the salicylaldehyde derivatives and HA were
139 evaluated from their absorption spectra at different pHs using the non-linear least-square Solver
140 program of Excel.

141

142 **Voltammetric measurements**

143 Square wave voltammetry (SWV) was performed by a BD-101 (Satoda Science, Japan).
144 A conventional three-electrode system was used with a glassy carbon (3-mm diameter, BAS, Japan),
145 Ag/AgCl (3 mol dm⁻³ NaCl, BAS, Japan), and platinum wire as the working, reference, and counter
146 electrodes, respectively. The SWV parameters were as follows: the frequency was 100 Hz, the
147 amplitude was 25 mV, and the step potential was 4 mV. The potential was scanned from -0.2 to -1.6
148 V (vs. Ag/AgCl).

149 For the kinetic study of the complexation, the time variation of the SWV signals was
150 observed. The 20 cm³ sample with or without 10 mg B dm⁻³ boric acid was used to investigate the
151 processes for the AzH and AzB formations. The reaction was started after adding the aldehyde

152 solution to the mixture containing the buffer solution and HA with or without boric acid. The
153 measurements were performed until the reaction reached equilibrium. The temperature was usually
154 set at 298 K. For the measurement to estimate the activation parameters, the temperature was
155 changed between 283 K and 303 K at 5 K intervals using a thermostated bath.

156 The concentration condition optimized in a previous study was employed for the
157 determination of boron in this study [26]. The solution was prepared by adding a 5 cm³ buffer
158 solution, 0.25 g HA, and 1 cm³ aldehyde solution to a 20 cm³ sample solution. The solution was
159 allowed to stand for 5 min before the SWV measurement after mixing these reagents. A calibration
160 curve was prepared in the range between 0 and 10 mg B dm⁻³ boric acid.

161 A curve fitting program was used to separate the peak of the AzB complex from the other
162 peaks for the SWV measurements. Allowing for an appropriate baseline, the shape of each peak
163 was symmetric with respect to the applied potential. Therefore, the pseudo-Voigt function, which is
164 a linear combination of the Lorentz and Gauss functions, was applied to the curve fitting (Fig. S1 in
165 the ESI).

166

167 **NMR measurements**

168 ¹¹B NMR measurements were performed using a JEOL JNM-ECX400 spectrometer at a
169 resonance frequency of 128.3 MHz with 10-mm multinuclear probe at 296 K. The field frequency
170 lock was achieved with the deuterium resonance of D₂O in a concentric capillary tube. The
171 chemical shifts were referenced with respect to an external BF₃-OEt₂ standard at 0.0 ppm. On this
172 scale, the signal of boric acid occurs at 19.4 ppm. The standard NMR parameters were as follows:
173 the flip angle was *ca.* 90° (28 μs), the pulse repetition time was 1s, and the spectral width was 22
174 kHz. The sample solutions (the ionic strength was 0.5 mol dm⁻³, NaCl) containing known amounts
175 of boric acid/borate and ligands were prepared, and the pHs were adjusted with the buffer solutions.
176 After being allowed to stand for about 100 min, the solutions were used for the NMR

177 measurements. A Lorentzian curve-fitting method was used to evaluate the individual signal
178 intensities.

179

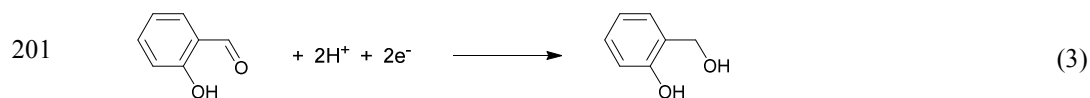
180 **Results and discussion**

181 **SWV peak potentials**

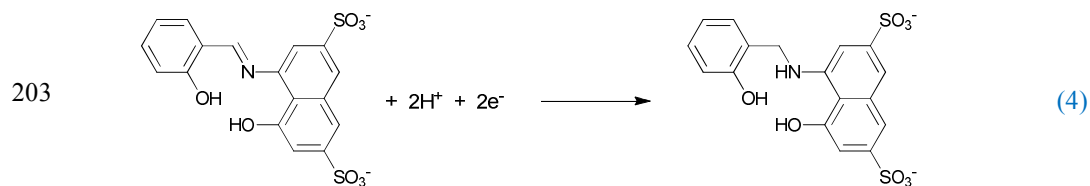
182 The following three solutions were prepared for the assignment of the SWV peaks: a 2.0
183 mmol dm⁻³ SA solution (pH 4.3), a 2.0 mmol dm⁻³ SA and 25 mmol dm⁻³ HA solution (pH 4.3) with
184 or without 10 mg B dm⁻³ boric acid. **Figure 1** shows the voltammograms of the SWV measurements
185 for these solutions. Only one peak was observed at -1.22 V in the solution containing only SA.
186 Thus, this peak can be assigned to the reduction of the free SA. For the solution containing SA and
187 HA without boric acid, another peak was observed at -0.92 V in addition to the SA peak. There
188 should be SA, HA, and AzH in the solution. Because HA is an electro-inactive species, the peak
189 can be assigned to the reduction of AzH. For the solution containing SA and HA with boric acid, a
190 third peak different from the SA and AzH peaks was observed at -1.04 V, and therefore, the peak at
191 -1.04 V was assigned to the reduction of AzB. In the same way, all peaks were assigned for each
192 system using F-SA or Me-SA.

193 Because protonation might be involved in the reduction process of SA, AzH, and AzB,
194 the effect of the solution pH on the SWV was examined (**Fig. 2**). The cathodic peak potentials of
195 both SA and AzH shifted to more negative potentials with the increasing pH. On the other hand, the
196 peak potential of AzB was scarcely affected by the pH change. Similar results were also obtained
197 for the F-SA and Me-SA systems. These results indicated that a proton participates in the case of
198 the SA and AzH reductions, which are shown in eqs (3) and (4). SA would be reduced to form the
199 salicylalcohol, and AzH would be reduced *via* the protonation of the C=N unit.

200



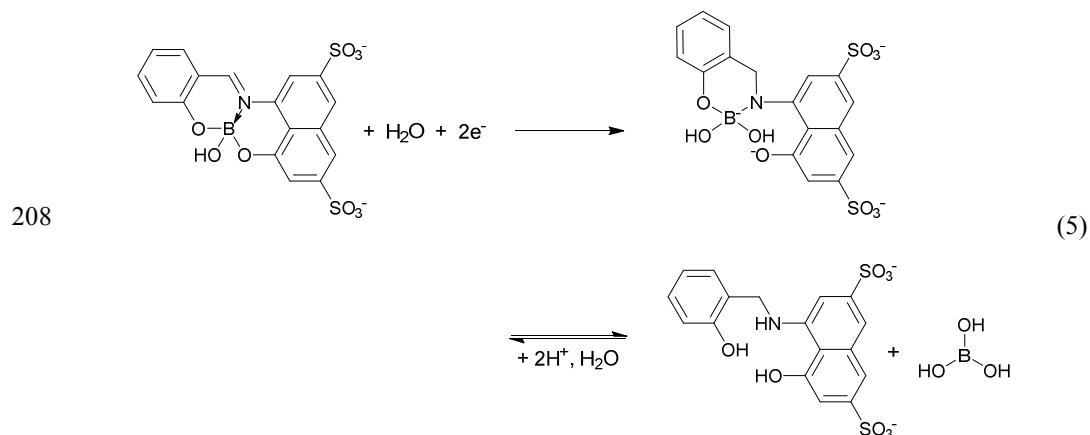
202



204

205 In contrast, because the peak potential of AzB is independent of the pH, the possible reaction may
206 be given in the first step of eq (5).

207



209

210 The effect of the substituent on the peak potentials was also examined (Fig. 2). The
211 cathodic peak potentials of the analogs differed depending on the aldehyde used at the same pH.
212 The fluoro group is known as an electron-withdrawing group and expected to decrease the electron
213 density of the reduction site. In fact, the peak potentials of the fluoro species became more positive
214 than the other analogs. On the other hand, the methyl group is a weak electron-donating group, and
215 the peak potentials of Me-SA were observed at a slightly more negative potential than SA. Because
216 the shift was small, the methyl group did not have a great influence on the peak potentials.

217 The peak area of the cathodic current was used to determine each concentration of the
 218 electroactive species, that is, SA, AzH and AzB, because the charge transfer steps of these
 219 compounds include the same number of electrons as shown by eqs (3), (4) and (5).

220

221 **Complexation equilibria of the boric acid-SA-HA system**

222 The formation constants for the AzH and AzB formations (K_{AzH} and K_{AzB}) are defined by
 223 the following equations:

$$224 \quad K_{AzH} = \frac{[AzH]}{[SA][HA]} \quad (6)$$

$$225 \quad K_{AzB} = \frac{[AzB]}{[SA][HA][B]} \quad (7)$$

226 where [SA], [HA], [AzH], [AzB], and [B] are the concentrations of the respective species. The
 227 K_{AzH} and K_{AzB} values affect the observed reduction peak intensity of each corresponding species.
 228 The higher the formation constant, the higher the peaks of AzH and AzB would be obtained.

229 The K_{AzH} and K_{AzB} were estimated by analyzing the reduction peaks obtained by the
 230 SWV measurements for the solutions with or without 10 mg B dm^{-3} . The reactions were completed
 231 in about 60 min. To estimate the K_{AzH} and K_{AzB} values, the peak area (S) of each species obtained by
 232 separating the peaks was used. Because a large excess amount of HA was added relative to those of
 233 SA and boric acid, the concentration of free HA can be assumed to be constant. Thus, K_{AzH} can be
 234 calculated by eq (8).

$$235 \quad K_{AzH} = \frac{S_{AzH}}{S_{SA} C_{HA}} \left(1 + \frac{K_a^{SA}}{a_{H^+}} \right) \left(\frac{a_{H^+}}{K_{a1}^{HA}} + 1 + \frac{K_{a2}^{HA}}{a_{H^+}} \right) \quad (8)$$

236 K_a^{SA} is the dissociation constant of SA defined by $K_a^{SA} = a_{H^+}[SA^-]/[SA]$, and K_{a1}^{HA} and K_{a2}^{HA}
 237 are the first and second dissociation constants of HA defined by $K_{a1}^{HA} = a_{H^+}[HA^-]/[HA^+]$ and
 238 $K_{a2}^{HA} = a_{H^+}[HA^{2-}]/[HA^-]$, where a_{H^+} is the hydrogen ion activity. All the equilibrium constants

239 involved in the AzH formation are presented in Fig. 3.

240 For the estimation of K_{AzB} , the mass balance equation for the concentrations of the boron
241 species is expressed as eq (9) in a pH range lower than the boric acid pK_a^B .

$$242 \quad [B] = C_B - [AzB] \quad (9)$$

243 By using the total peak area $S_T = S_{SA} + S_{AzH} + S_{AzB}$ and the total concentration of SA (C_{SA}), K_{AzB}
244 can be calculated by eq (10), because the charge transfer steps of these compounds include the
245 same number of electrons (See eqs (3) – (5)).

$$246 \quad K_{AzB} = \frac{S_{AzB}}{S_{SA} C_{HA} (C_B - (S_{AzB}/S_T) C_{SA})} \left(1 + \frac{K_a^{SA}}{a_{H^+}} \right) \left(\frac{a_{H^+}}{K_{al}^{HA}} + 1 + \frac{K_{a2}^{HA}}{a_{H^+}} \right) \quad (10)$$

247 The K_{AzH} values determined by voltammetry and the K_{AzB} values determined by voltammetry
248 (Tables S1 and S2 in the ESI) and ^{11}B NMR measurements are shown in Table 1. In the case of SA as
249 the aldehyde, Matsuo *et al.* reported that K_{AzH} is lower than 10 and K_{AzB} is $10^{5.91}$ ($I = 0.1$) [23].
250 These values are in fairly good agreement between the two methods. Among the examined analogs
251 of salicylaldehyde, Me-SA was found to produce the lowest K_{AzH} value. The K_{AzB} values were
252 similar among SA analogs, even though the value for Me-SA was a little lower than the others and
253 the formation constants of the reaction, $AzH + B \rightleftharpoons AzB$, corresponding to K_{AzB}/K_{AzH} , were almost
254 the same, which suggested that there are no differences in the free energy changes between AzB and
255 AzH for the three aldehyde analogs.

256

257 Kinetic study on the boric acid-SA-HA system

258 The time variation of the SWV signals was observed using the solutions with or without
259 10 mg B dm^{-3} boric acid. The AzH and AzB formation processes were observed at pH 4.3 and 7.5 –
260 7.7. Figure 4 shows the voltammograms of the SWV measurements for the solutions containing SA
261 and HA without boric acid. The peak intensity of AzH became constant within 10 min at pH 4.3,
262 whereas it took about 30 min at pH 7.5. For this reason, the formation rate of AzH depended on the

263 pH and that the rate was higher at the low pH. Similar SWV peak trends were also observed at the
 264 SWVs of the F-SA and Me-SA species (Fig. S2 in the ESI). Generally, it is known that Schiff-base
 265 formation is catalyzed by protons. The pH dependence of the formation rates for various
 266 Schiff-bases was reported. For example, the formation reaction of *N-p*-chlorobenzylidene aniline
 267 became faster with the decreasing pH in the range of pH 4 to 6 [27], which is similar to the results
 268 obtained in this study.

269 Figure 5 shows the voltammograms of the SWV measurements for the solutions
 270 containing SA, HA and 10 mg B dm⁻³ boric acid. In this case, the pH dependence of the AzB
 271 formation rate was also observed. The peak intensities of AzB and its analogs increased for 40 min
 272 at pH 4.3, while they became constant within 10 min at pH 7.5 – 7.7. Contrary to the AzH
 273 formation, the rate of AzB was higher under a neutral condition than under an acidic condition.

274 In order to quantitatively discuss the substituent effect for the AzB complexation reaction,
 275 we estimated the rate constants for the reaction by analyzing in detail the voltammograms of the
 276 solution containing 10 mg B dm⁻³ boric acid. Equation (11) is the third-order rate equation of the
 277 overall reaction of the formation of AzB from SA, HA, and boric acid.

$$278 \quad v = \frac{d[\text{AzB}]}{dt} = k_{\text{app}}[\text{B}][\text{SA}][\text{HA}] \quad (11)$$

279 This rate constant is defined as the apparent rate constant (k_{app}), and was experimentally obtained
 280 here (Table 2). Because a large excess amount of HA was added, eq (11) can be approximated by
 281 the pseudo-second order equation. At pH 4.3, the AzH formation is fast, so it was considered that
 282 the reaction had already reached equilibrium in the measured time period. Equation (11) can then
 283 be converted to eq (12) using the mass balance equations.

$$284 \quad \frac{d[\text{AzB}]}{dt} = k_{\text{app}} \cdot \frac{C_{\text{HA}}(C_{\text{SA}} - [\text{AzB}])(C_{\text{B}} - [\text{AzB}])}{(a_{\text{H}^+}/K_{\text{al}}^{\text{HA}} + 1)(1 + K_{\text{AzH}}C_{\text{HA}}/(a_{\text{H}^+}/K_{\text{al}}^{\text{HA}} + 1))} \quad (12)$$

285 Equation (13) is obtained by solving eq (12). The apparent rate constants were calculated from the

286 slope of the plot of eq (13) (Fig. S3 in the ESI).

$$287 \quad \ln \frac{C_B(C_{SA} - [AzB])}{C_{SA}(C_B - [AzB])} = k_{app} \cdot \frac{C_{HA}(C_{SA} - C_B)}{(a_{H^+}/K_{a1}^{HA} + 1)(1 + K_{AzH}C_{HA}/(a_{H^+}/K_{a1}^{HA} + 1))} \cdot t \quad (13)$$

288 At pH 7.6, in contrast, the rate constant could not be calculated in the way as stated above, because
 289 the AzH formation reaction became slower under this pH condition. Although the best approach is to
 290 consider two parallel reactions of the AzH and AzB formations, the rate equation is too complicated
 291 to solve in this case. Thus, we approximately estimated k_{app} at pH 7.6 as follows. The [SA] and [HA]
 292 were approximated with their initial concentrations using only the results during the initial reaction
 293 time of 150 s, in which the consumption of SA and HA was only 15%. Thus, Equation 12 can be
 294 converted as follows:

$$295 \quad \frac{d[AzB]}{dt} = \frac{k_{app}C_{HA}C_{SA}(C_B - [AzB])}{(1 + K_{a2}^{HA}/a_{H^+})(1 + K_a^{SA}/a_{H^+})} \quad (14)$$

$$296 \quad \ln(C_B - [AzB]) = -\frac{k_{app}C_{HA}C_{SA}}{(1 + K_{a2}^{HA}/a_{H^+})(1 + K_a^{SA}/a_{H^+})} \cdot t + \ln C_B \quad (15)$$

297 The apparent rate constants were calculated from the slope of the plot of eq (15) (Fig. S4 in the
 298 ESI). As shown in Table 2, the rate constants at pH 7.6 were somewhat higher than those at pH 4.3.
 299 However, if HA and HA⁻ are assumed to have the same reactivity, they were almost the same for
 300 each analog. The k_{app} values varied with the aldehydes used in the order of F-SA > SA ≈ Me-SA.
 301 Therefore, it is indicated that the fluoro group is kinetically-favored for the AzB complexation.

302 The effect of the temperature on the apparent rate constant was investigated in the range
 303 of 283 – 303 K. The activation parameters were calculated by the Eyring equation (eq (16)).

$$304 \quad \ln \frac{k_{app}}{T} = -\frac{\Delta H^\ddagger}{RT} + \ln \frac{k_B}{h} + \frac{\Delta S^\ddagger}{R} \quad (16)$$

305 where R is the gas constant, T the absolute temperature, k_B the Boltzmann constant, and h Planck's
 306 constant (Fig. S5 in the ESI). The obtained data are summarized in Table 3. The lowest activation

307 enthalpy change was found for F-SA as the aldehyde. The activation entropy changes were negative
308 in all the investigated analogs. A slightly lower activation free energy change was observed for
309 F-AzB than for the other analogs. For the contribution to the activation free energy, it was found
310 that the contribution of the activation entropy changes is much higher than that of the activation
311 enthalpy changes.

312

313 **Boric acid-SA-HA complexation mechanism**

314 Summarizing the above information, we now propose the reaction mechanisms of the
315 AzB formation. The formation reactions of AzH were faster at a lower pH in the cases using any
316 aldehydes. The conditions at pH 4.3 and 7.5 – 7.7 used in this study are sensitive to the acid
317 dissociation of SA and HA, as shown in Fig. 3. AzH originates by nucleophilic attack of the
318 nitrogen atom of the amino group in HA on the formyl group in SA. This reaction would be
319 accelerated using an aldehyde with a higher electrophilicity. SA is stabilized by the intramolecular
320 hydrogen bond, which should contribute to the decrease in the electron density of the carbon atom.
321 It is expected that the dissociated SA (SA^-) and protonated HA (HA^+) are not involved in the AzH
322 formation [28].

323 In the case of the AzB formation reaction, the main process of the AzB complexation
324 from SA, HA, and boric acid is considered to consist of more than three steps [29]: (1) the
325 pre-equilibrium of the boric acid-salicylaldehyde complex (SA-B) formation, (2) the nucleophilic
326 attack of HA to SA-B affording the zwitterionic intermediate, and (3) some remaining steps to form
327 AzB including proton transfers, the elimination of a water and intramolecular dehydration between
328 the hydroxy group in the boric acid moiety and the phenolic hydroxyl group in the HA moiety (Fig.
329 6). Although it is likely that AzH directly reacts with boric acid, this reaction path should not be the
330 main process because the kinetics of the AzH and AzB formations exhibited the opposite
331 characteristics to the pH. It is expected that the electron density of the formyl group is decreased by

332 the SA-B formation in a way similar to the intramolecular hydrogen bond of SA. The subsequent
333 nucleophilic attack of HA on SA-B easily takes place, and the reaction affords the
334 thermodynamically stable AzB complex even under the conditions of a higher pH at which the
335 activation by protonation is not expected.

336 By considering the proposed mechanism, eq (11) can also be converted to the intrinsic
337 rate equation as follows:

338
$$v = \frac{d[\text{AzB}]}{dt} = k_{\text{app}}[\text{B}][\text{SA}][\text{HA}] = k[\text{SA} - \text{B}][\text{HA}] \quad (17)$$

339 where k is the intrinsic rate constant of the reaction between SA-B and HA. Therefore, the apparent
340 rate constant obtained in this study can be expressed using $K_{\text{SA-B}}$, *i.e.*, $k_{\text{app}} = k \cdot K_{\text{SA-B}}$. However, it
341 was difficult to determine $K_{\text{SA-B}}$; the interaction between SAs and boric acid could not be
342 confirmed by the ^{11}B NMR measurements because of very low solubilities of SAs in water and low
343 $K_{\text{SA-B}}$ nor by absorption spectra measurements in a UV region because of their similar absorption
344 spectra of the free SAs and SA-B and low $K_{\text{SA-B}}$.

345 The initial aldehyde concentration might affect the observed results from the kinetic
346 experiments. Because C_{SA} was limited to about one-tenth of C_{HA} to reduce the overlap of the
347 reduction peaks [26], the AzH and SA-B formation reactions are considered to have competitively
348 proceeded. At pH 4.3, SA would be consumed by the AzH formation because the reaction was
349 faster at this pH. Due to the slow reaction between AzH and boric acid, it took a longer time to
350 attain the equilibrium for the AzB formation from them. On the other hand, because the AzH
351 formation was slower at pH 7.5 – 7.7, SA might be scarcely consumed by the AzH formation
352 during the initial stage of the reaction. From the viewpoint of the AzB formation, it is expected that
353 the concentration of SA, which can be used for the reaction, was different depending on the pH.

354

355 **Analytical application to voltammetric determination of boron**

356 From a practical point of view, the formation constants and rate constants are related to the
357 peak intensities of the target complex and measurement time, respectively. As already mentioned,
358 the AzB complexation rate, which alters in accordance with the pH, is faster around the neutral
359 region. For this reason, it is better to measure the boron concentration in the neutral region. The K_{AzB}
360 values are similar among the SA analogs, which produces no difference in the sensitivity among the
361 three kinds of SAs. It is also better for practical use that the AzB peak is separated from the other
362 peaks, in particular, from SA, because its peak has the highest intensity. The cathodic peaks of AzB,
363 AzH, and SA were observed in a close potential range, while the peak potentials of AzH and SA
364 were affected by both the pH and the substituents. It was found that the peaks of SA and AzH shifted
365 to negative potentials with the increasing pH, whereas the peak potential of AzB scarcely changed
366 with the pH (Fig. 2). With the increasing pH, the separation of peaks would be better, however, the
367 AzB complexation degree should decrease over pH 8 due to the acid dissociation of SA. Thus, it is
368 reasonable to determine the boron concentration under a neutral condition. In this study, the
369 determination of boron was performed at $\text{pH } 7.5 \pm 0.1$. Under this pH condition, F-SA showed the
370 best separation between the AzB and AzH peaks (Fig. 5), and was chosen as the aldehyde.

371 The effect of foreign ions is shown in Table 4. In the case of the phosphate buffer,
372 insoluble salts were formed with the calcium and magnesium ions. Thus, the HEPES buffer was
373 used instead of the phosphate buffer. The HEPES buffer exhibited no influence in the scanned
374 potential range. Copper interfered with the boron determination by the proposed method if present
375 in 2 times higher concentrations than that of boric acid (Fig. S6 in the ESI). For the other examined
376 ions, it was confirmed that the amounts of coexisting ions normally present in seawater and
377 desalinated water are tolerable. In addition, the proposed method can be sufficiently applied to
378 industrial effluents. If samples contain more than 1 mg dm^{-3} copper, pretreatment using a chelate
379 resin column, such as InertSep ME-1 (GL Science, Tokyo, Japan), was effective in order to remove
380 the copper.

381 Under the optimized conditions, the AzB peak could be observed within 5 min and was
382 proportional to the boron concentration (Fig. 7). In order to make a calibration curve for practical
383 use, the following parameters were defined: E_{peak} is the peak potential of AzB; E_{base} is the baseline
384 potential outside the peak; I_{peak} and I_{base} are the respective currents at E_{peak} and E_{base} . A calibration
385 curve was made for the difference between I_{peak} and I_{base} versus the boron concentration: $\Delta I / \mu\text{A} =$
386 $I_{\text{peak}} / \mu\text{A} - I_{\text{base}} / \mu\text{A} = -1.075 C_{\text{B}} / \text{mg dm}^{-3} - 0.400$ ($R^2 = 0.999$), where C_{B} is the boric acid
387 concentration. In this study, E_{peak} was observed at -0.96 V, and E_{base} was set to -0.50 V. The limit of
388 detection, which is defined as the concentration that gives a current corresponding to 3σ for the
389 standard deviation of the fluctuation of the blank, was $0.03 \text{ mg B dm}^{-3}$ ($n = 5$). This limit of
390 detection is better than the value (0.1 mg B dm^{-3}) obtained in a previous study [26].

391 The recovery test was also made using the standard addition method. This test was applied
392 to the samples of seawater and the water from a desalination plant using reverse osmosis (RO). All
393 the samples were 5 times diluted. The recoveries were nearly 100% for all the examined water
394 samples (Table 5).

395 The proposed SWV method was used to determine the boron concentration in seawater,
396 RO water from a desalination plant, and industrial effluent samples. The results are summarized in
397 Table 6. For all the water samples measured, the boron concentrations determined by the SWV
398 method were in good agreement with those determined by the conventional spectroscopic methods
399 having differences of less than 10%. These results prove the validity of the proposed method. In the
400 case of the samples with a high ionic strength over 1, direct measurements without dilution resulted
401 in about -20% differences. However, the problem was solved by measuring after a 5 times dilution.

402

403 **Conclusion**

404 The reaction of the AzB complexation has been practically applied to the determination of boron
405 concentrations in solution using absorption spectrophotometry and voltammetry. Nevertheless, its

406 reaction mechanism has not been studied in detail for a long time as it is a ternary complex system.
407 In this study, the AzB complexation mechanism was completely clarified from kinetic and
408 equilibrium points of view using SWV and ^{11}B NMR measurements. F-SA and Me-SA were helpful
409 to clarify the effect of the substituent groups.

410 Based on the full knowledge of this system, the boron determination system using SWV,
411 which has been proposed in our laboratory, was optimized. The peak potentials of AzH and SA
412 were shifted negative with the increasing pH, while that of AzB was pH-independent. Because a
413 neutral condition is favorable from the viewpoints of the AzB formation rate and peak potentials,
414 the measurements were performed at $\text{pH } 7.5 \pm 0.1$. In addition, F-SA was chosen because it showed
415 a better peak separation. The proposed method enabled the determination of a lower boron
416 concentration in a shorter time than the previous method. This method is simple, rapid and easy to
417 operate, and can be applied to samples, such as seawater, RO water, and some industrial effluents.
418 The information obtained in this study is also expected to be applied to the boron determination
419 using absorption spectrophotometry, which will be reported elsewhere [30].

420

421 **Acknowledgements**

422 The authors would like to express their sincere thanks to Mr. Takamasa Kodani of Kyushu
423 University and Mr. Hiroyuki Mabuchi of National Institute of Technology, Miyakonojo College for
424 their useful experimental support. They also thank the Fukuoka District Water Agency
425 Desalination Center “Mamizu-pia” for the donation of the RO water samples. This work was
426 partially supported by Takaoka Chemical Company, Ltd.

427

428 **References**

429 [1] F. A. Cotton, G. W. Wilkinson, C. A. Murillo and M. Bochmann, *Advanced Inorganic*
430 *Chemistry*, 6th ed., Wiley-Interscience, New York (1999).

- 431 [2] M. van Duin, J. A. Peters, A. P. G. Kieboom and H. van Bekkum, *Tetrahedron*, 1985, **41**,
432 3411-3421.
- 433 [3] J. G. Dawber and S. I. E. Green, *J. Chem. Soc., Faraday Trans. 1*, 1986, **82**, 3407-3413.
- 434 [4] R. Pizer, P. J. Ricatto and C. A. Tihal, *Polyhedron*, 1993, **12**, 2137-2142; R. Pizer and P. J.
435 Ricatto, *Inorg. Chem.*, 1994, **33**, 2402-2406.
- 436 [5] Y. Miyazaki, K. Yoshimura, Y. Miura, H. Sakashita and K. Ishimaru, *Polyhedron*, 2003, **22**,
437 909-916.
- 438 [6] Y. Miyazaki, T. Fujimori, H. Okita, T. Hirano and K. Yoshimura, *Dalton Trans.*, 2013, **42**,
439 10473-10486.
- 440 [7] C. Shao, S. Matsuoka, Y. Miyazaki, K. Yoshimura, T. M. Suzuki and D. A. Tanaka, *J. Chem.*
441 *Soc., Dalton Trans.*, 2000, **18**, 3136-3142.
- 442 [8] C. Shao, S. Matsuoka, Y. Miyazaki and K. Yoshimura, *Anal. Sci.*, 2001, **17** (Supplement),
443 i1475-i1478.
- 444 [9] Y. Miyazaki, H. Matsuo, T. Fujimori, H. Takemura, S. Matsuoka, T. Okobira, K. Uezu and K.
445 Yoshimura, *Polyhedron*, 2008, **27**, 2785-2790.
- 446 [10] K. C. Berger and E. Truog, *Ind. Eng. Chem. Anal. Ed.*, 1939, **11**(10), 540-545.
- 447 [11] J. M. Conner and V. C. Bulgrin, *J. Inorg. Nucl. Chem.*, 1967, **29**, 1953-1961.
- 448 [12] N. Geffen, R. Semiat, M. S. Eisen, Y. Balazs, I. Katz and C. G. Dosoretz, *J. Membrane Sci.*,
449 2006, **286**, 45-51.
- 450 [13] K. Yoshimura, Y. Miyazaki, S. Sawada and H. Waki, *J. Chem. Soc., Faraday Trans.*, 1996, **92**,
451 651-656.
- 452 [14] C. Shao, Y. Miyazaki, S. Matsuoka, K. Yoshimura and H. Sakashita, *Macromolecules*, 2000,
453 **33**, 19-25.
- 454 [15] K. Yoshimura, Y. Miyazaki, F. Ota, S. Matsuoka and H. Sakashita, *J. Chem. Soc., Faraday*
455 *Trans.*, 1998, **94**(5), 683-689.

- 456 [16] C. Shao, S. Matsuoka, Y. Miyazaki and K. Yoshimura, *Analyst*, 2002, **127**(12), 1614-1620.
- 457 [17] R. N. Sah and P. H. Brown, *Microchem. J.*, 1997, **56**, 285-304.
- 458 [18] K. Yoshimura, Y. Miyazaki, S. Matsuoka, K. Takehara and T. Fujimori, in *Handbook of*
459 *Inorganic Chemistry Research* (Ed: D. A. Morrison), Nova Science Publishers, New York,
460 2010, 173 -209.
- 461 [19] R. Capelle, *Anal. Chim. Acta*, 1964, **24**, 555-572.
- 462 [20] K. L. Tu, L. D. Nghiem and A. R. Chivas, *Separation and Purification Technology*, 2010, **75**,
463 87-101.
- 464 [21] P. P. Power and W. G. Woods, *Plant and Soil*, 1997, **193**, 1-13; R. O. Nable, G. S. Banuelos and
465 J. G. Paull, *ibid.*, 1997, **193**, 181-198; F. H. Nielsen, *ibid.*, 1997, **193**, 199-208.
- 466 [22] V. M. Dembitsky, R. Smoum, A. A. Al-Quntar, H. A. Ali, I. Pergament and M. Srebnik, *Plant*
467 *Science*, 2002, **163**, 931-942.
- 468 [23] H. Matsuo, Y. Miyazaki, H. Takemura, S. Matsuoka, H. Sakashita and K. Yoshimura,
469 *Polyhedron*, 2004, **23**, 955-961.
- 470 [24] D. L. Harp, *Anal. Chim. Acta*, 1997, **346**, 373-379.
- 471 [25] T. Fujimori, H. Akimoto, Y. Tsuji, K. Takehara and K. Yoshimura, *Electroanalysis*, 2010,
472 **22**(12), 1337-1343.
- 473 [26] K. Takehara, T. Fujimori, K. Inagi, M. Kajiwara, Y. Harata and K. Yoshimura, *Electroanalysis*,
474 2013, **25**(2), 387-393.
- 475 [27] E. H. Cordes and W. P. Jencks, *J. Am. Chem. Soc.*, 1962, **84**, 832-837.
- 476 [28] C. Godoy-Alcántar, A. K. Yatsimirsky and J. -M. Lehn, *J Phys. Org. Chem.*, 2005, **18**,
477 979-985.
- 478 [29] N. E. Hall and B. J. Smith, *J. Phys. Chem. A*, 1998, **102**, 4930-4938.
- 479 [30] Sarenqiqige, T. Kodani, M. Kajiwara, K. Takehara and K. Yoshimura, *Anal. Sci*, 2014, **30**(9),
480 885-889.

482 Figure captions

483

484 **Fig. 1** SWVs of a 2.0 mmol dm⁻³ SA solution, and 2.0 mmol dm⁻³ SA and 25 mmol dm⁻³ HA
485 solutions with or without 10 mg B dm⁻³ (pH 4.3).

486

487 **Fig. 2** pH dependence of peak potentials for 25 mmol dm⁻³ HA solutions containing 2.0
488 mmol dm⁻³ (a) SA, (b) F-SA or (c) Me-SA with or without 10 mg B dm⁻³.

489

490 **Fig. 3** AzH formation equilibrium and the acid dissociation of the starting materials.

491

492 **Fig. 4** Dependence of SWVs on reaction time for AzH formation in solutions containing 2.0
493 mmol dm⁻³ SA and 25 mmol dm⁻³ HA at (a) pH 4.3 and (b) pH 7.5.

494

495 **Fig. 5** Dependence of SWVs on reaction time for AzB formation in solutions containing 2.0
496 mmol dm⁻³ SA analog, 25 mmol dm⁻³ HA and 10 mg B dm⁻³. AzB: (a) pH 4.3, (b) pH 7.5;
497 F-AzB: (c) pH 4.3, (d) pH 7.7; Me-AzB: (e) pH 4.3, (f) pH 7.7.

498

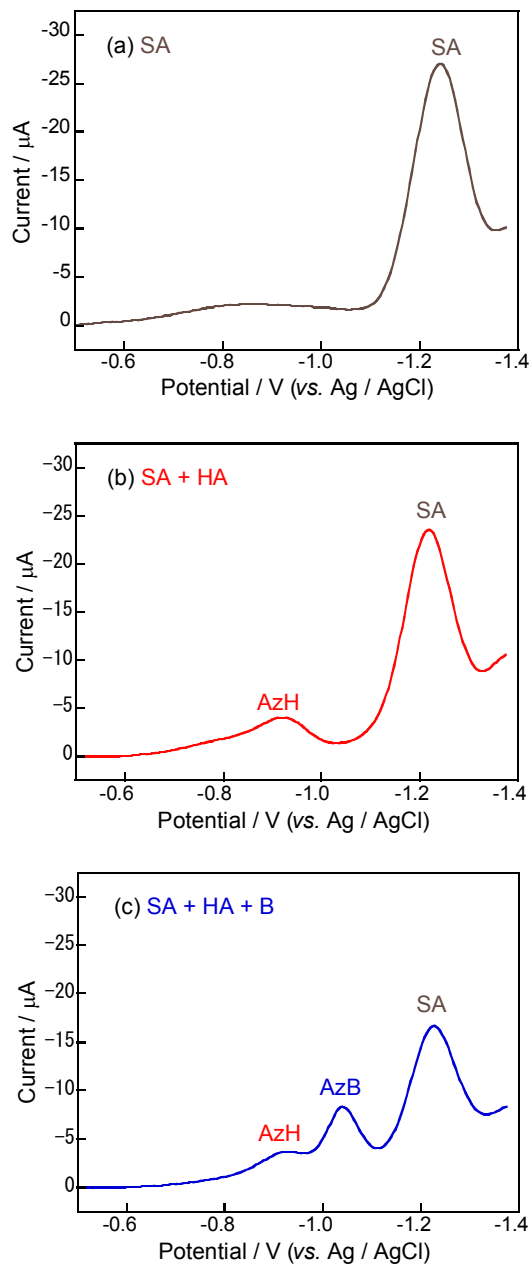
499 **Fig. 6** Plausible energy diagram for AzB formation from SA, B and HA. The energy
500 diagram for subsequent reactions of zwitterionic intermediate formation was simplified.

501

502 **Fig. 7** Dependence of SWVs on the boron concentration for the F-AzB formation system at
503 pH 7.5 ± 0.1. Concentrations of SA and HA are 2.0 mmol dm⁻³ and 25 mmol dm⁻³.

504

505



506

507

508

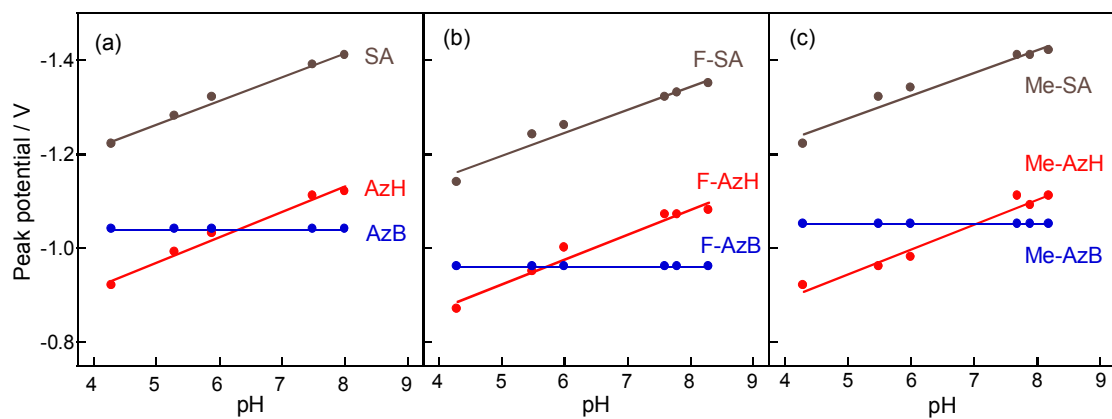
509

510

511 Fig. 1.

512

513



514

515

516

517

518

519

520

521

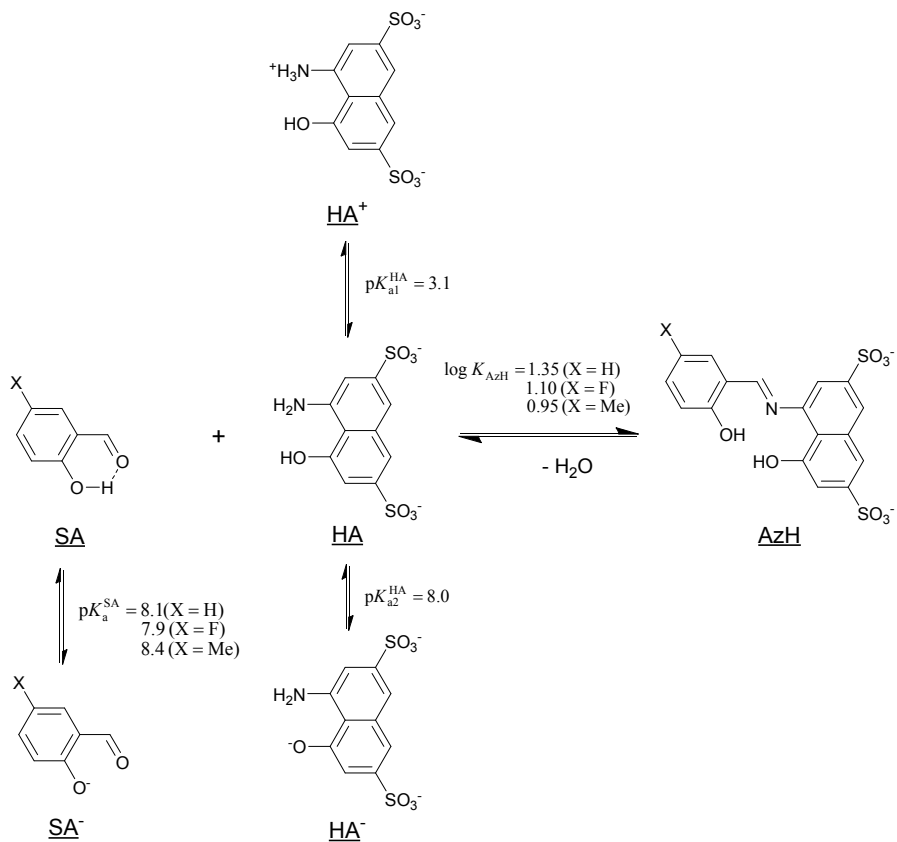
522 Fig. 2

523

524

525

526



527

528

529

530

531

532

533

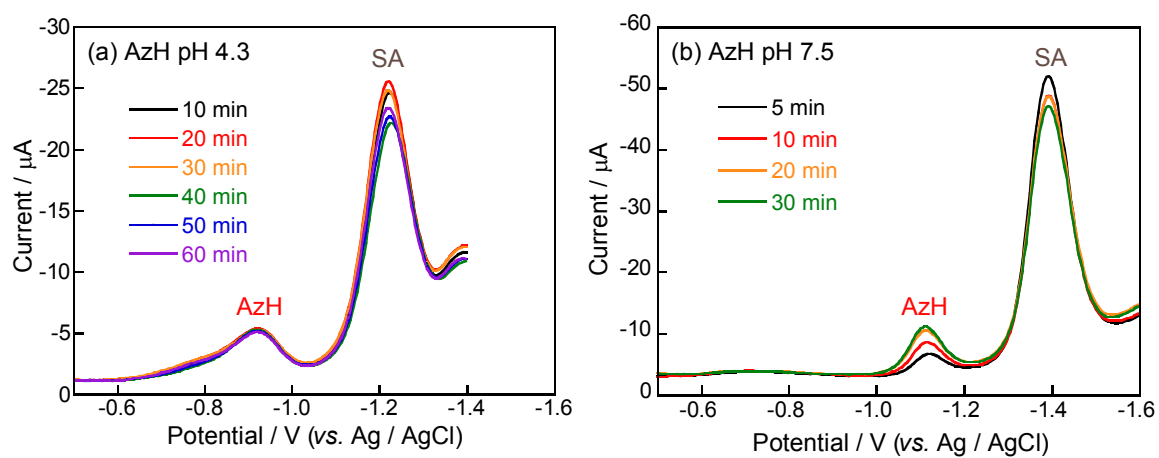
534

535 Fig. 3

536

537

538



539

540

541

542

543

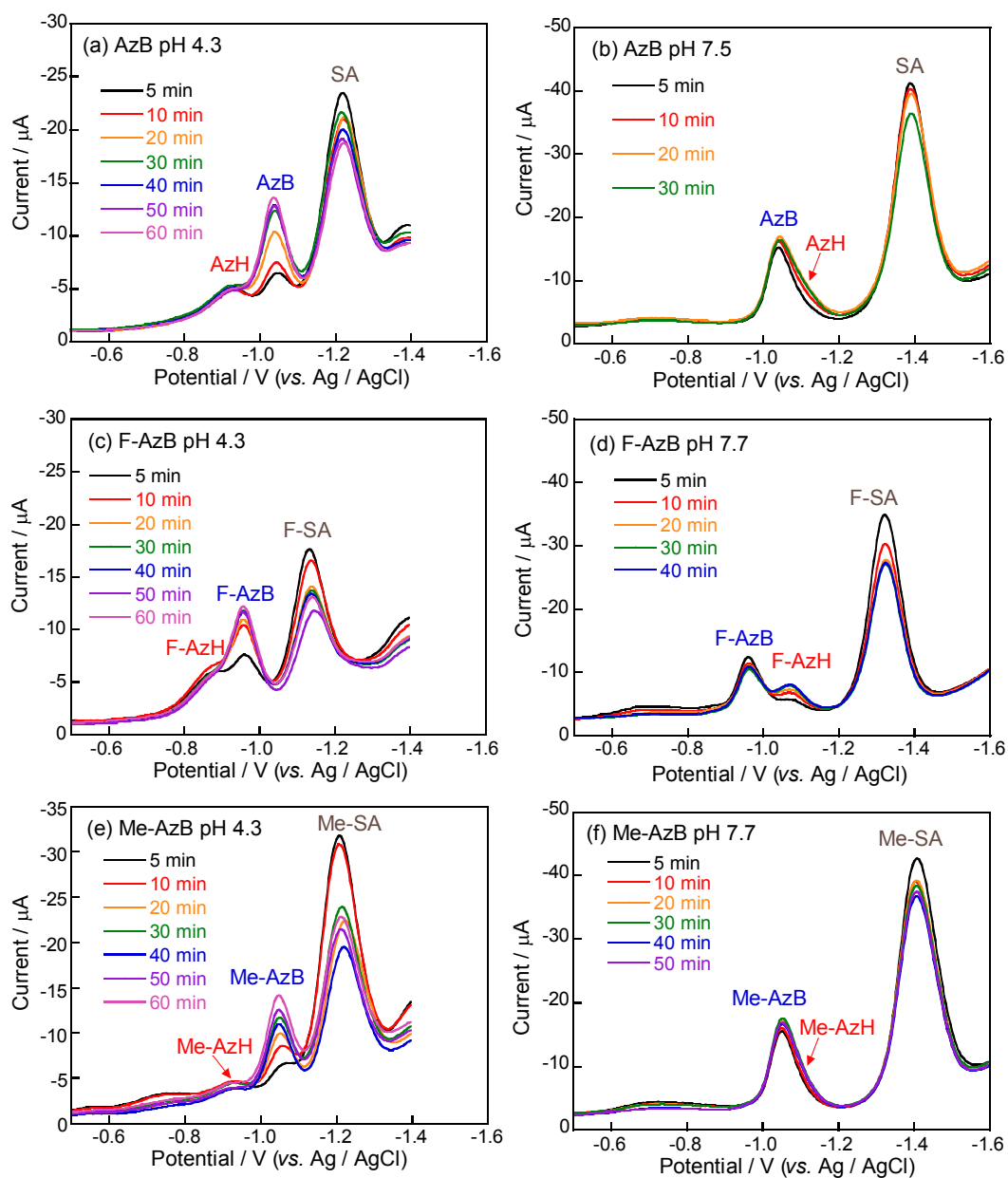
544

545

546

547 Fig. 4

548



549

550

551

552

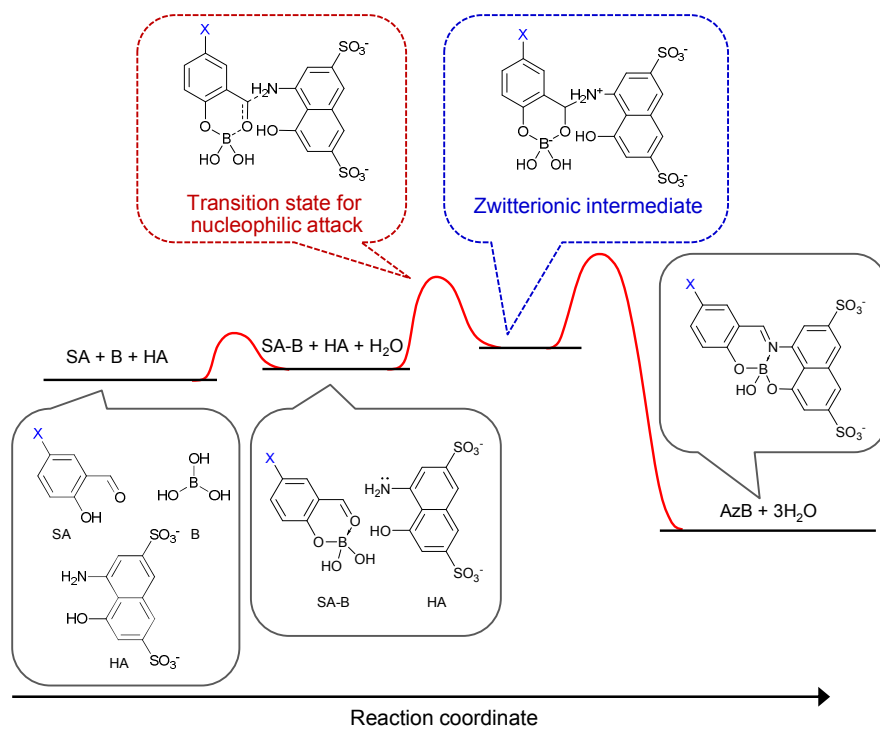
553 Fig. 5

554

555

556

557



558

559

560

561

562

563

564 Fig. 6

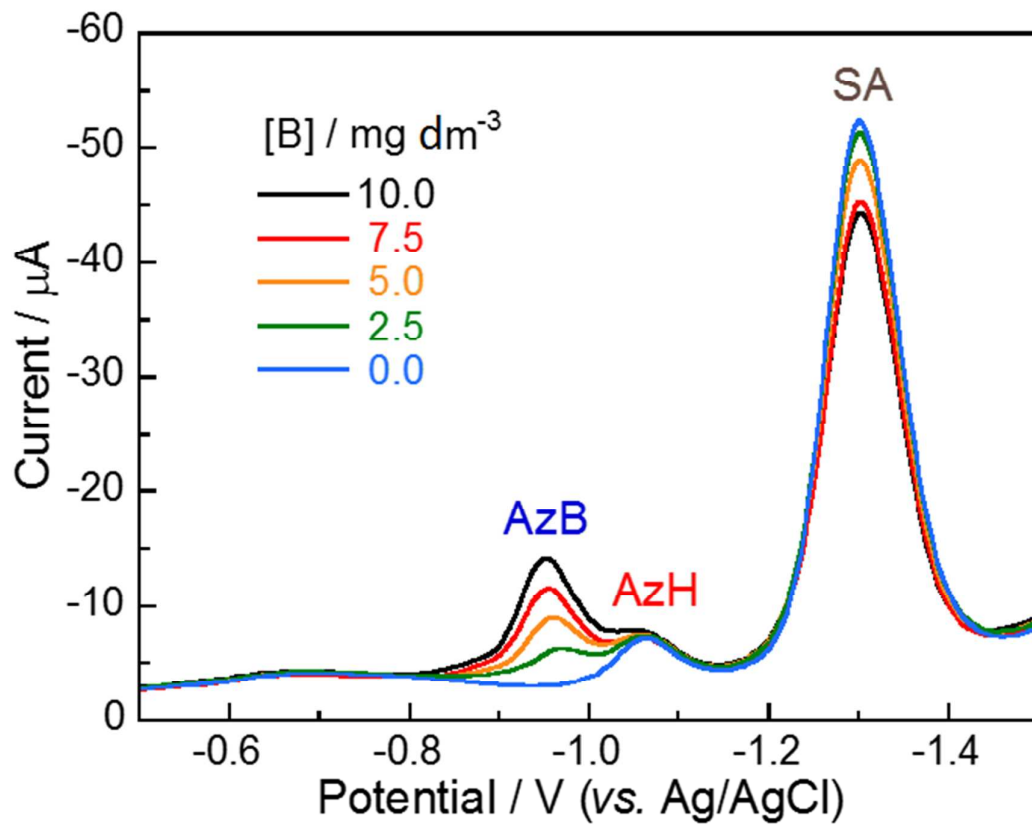
565

566

567

568

569



570

571

572

573

574

575

576 Fig. 7

577

578

579 Table 1. Formation constants of AzH and AzB for SA and its analogs ($I = 0.5$)

Aldehyde	Voltammetry			^{11}B NMR		
	pH	$\log(K_{\text{AzH}} / \text{mol}^{-1} \text{dm}^3)$	$\log(K_{\text{AzB}} / \text{mol}^{-2} \text{dm}^6)$	pH	$\log(K_{\text{AzB}} / \text{mol}^{-2} \text{dm}^6)$	
SA	4.3	0.99 ± 0.01	5.20 ± 0.03	4.5	5.38	
				5.3	5.16	$5.24 \pm 0.14^{\text{a}}$
				6.0	5.14	
F-SA	4.3	1.04 ± 0.00	5.35 ± 0.03	4.5	5.03	
				5.3	4.97	5.01 ± 0.03
				6.3	5.02	
Me-SA	4.3	0.70 ± 0.01	4.97 ± 0.02	4.4	5.36	
				5.2	5.15	5.22 ± 0.14
				6.1	5.11	

580 ^a 5.91 ± 0.07 ($I = 0.1$) [23]

581

582

583 Table 2. Rate constants for the AzB complexation among B, HA, and SA or its analogs at 298 K

584

Aldehyde	pH	$k_{\text{app}} / \text{mol}^{-2} \text{dm}^6 \text{s}^{-1}$
SA	4.3	22 ± 0
		$38 \pm 4^{\text{a}}$
	7.6	$30 \pm 3^{\text{b}}$
F-SA	4.3	62 ± 2
		$76 \pm 3^{\text{a}}$
	7.6	$59 \pm 3^{\text{b}}$
Me-SA	4.3	14 ± 0
		$43 \pm 2^{\text{a}}$
	7.6	$34 \pm 2^{\text{b}}$

585 ^a HA is assumed to be the only active species.

586 ^b HA and HA⁻ are assumed to be the active species.

587

588

589

590 Table 3. Activation parameters for the AzB complexation from B, HA, and SA or its analogs at

591 pH 4.3

	$\Delta H^{\ddagger} / \text{kJ mol}^{-1}$	$\Delta S^{\ddagger} / 10 \text{ J K}^{-1} \text{ mol}^{-1}$	$\Delta G^{\ddagger} / \text{kJ mol}^{-1}$
SA	10.2 ± 0.9	-18 ± 3	$63 \pm 9^{\text{a}}$
F-SA	6.7 ± 0.1	-19 ± 1	$62 \pm 2^{\text{a}}$
Me-SA	11.6 ± 0.6	-18 ± 2	$65 \pm 5^{\text{a}}$

^a Calculated as $\Delta G^{\ddagger} = \Delta H^{\ddagger} - T\Delta S^{\ddagger}$ at $T = 298 \text{ K}$.

592

593

Table 4. Effects of foreign ions on the determination of boron

	Coexisting ion / mg dm ⁻³	Found B / mg dm ⁻³	Relative error, %
Ca ²⁺	1000	5.09	+1.8
Mg ²⁺	1000	5.30	+5.9
Al ³⁺	100	5.06	+2.8
Fe ³⁺	100	5.04	+2.1
Pb ²⁺	100	4.90	-1.8
Zn ²⁺	100	5.29	+5.4
F ⁻	100	4.80	-3.2
Cu ²⁺	10	7.12	+42.9
	1	5.22	+4.7

(5 mg B dm⁻³)

594

595

596 Table 5. Recovery test of boron using standard addition

Sample	B added / mg dm ⁻³	B found / mg dm ⁻³	Recovery, %
ISW	0.00	0.86 ± 0.01 (<i>n</i> = 3)	–
	2.51	3.32	98
	5.00	5.88	100
REW	0.00	1.50 ± 0.02 (<i>n</i> = 3)	–
	2.50	3.93	97
	4.97	6.28	96
BHRO	0.00	1.68 ± 0.02 (<i>n</i> = 3)	–
	2.50	4.15	99
	5.00	6.54	97

ISW: Intake seawater; REW: RO effluent water; BHRO: Brine from high pressure RO.

597

598

599

600 Table 6. Boron concentrations of waters from a RO desalination plant and an industrial
 601 wastewater treatment plant

Sample	Ionic strength	SWV ^a / mg dm ⁻³	ABS ^b / mg dm ⁻³
RO desalination			
PLRO	4.1×10^{-3}	0.82 ± 0.01	0.77
PW	1.7×10^{-3}	1.23 ± 0.08	1.33
PHRO	2.0×10^{-3}	1.61 ± 0.03	1.59
FLRO	4.6×10^{-3}	2.99 ± 0.03	2.85
UFF	0.59	4.74 ± 0.08	4.68
ISW	0.59	4.64 ± 0.05	4.46
REW	1.1	5.94^c	7.19
		7.14 ± 0.08^d	
BHRO	1.3	6.62^c	8.05
		7.98 ± 0.07^d	
Industrial wastewater treatment			
After	< 0.1	0.09 ± 0.03	0.08^f
Before	< 0.1	13.0 ± 0.4^e	13^f

PLRO: Permeate low pressure RO; PW: Product water; PHRO: Permeate high pressure RO;
 FLRO: Feed for low pressure RO; UFF: UF filtrate; ISW: Intake seawater; REW: RO effluent
 water; BHRO: Brine from high pressure RO.

^a Proposed SWV method ($n = 3$);

^b Conventional Azomethine H absorption spectrophotometry;

^c No dilution; ^d 5 times dilution; ^e 2 times dilution; ^f ICP-AES.

602